Research Article

Structure-Property Relationship of New Organic Sensitizers Based on Multicarbazole Derivatives for Dye-Sensitized Solar Cells

Hyo Jeong Jo, Jung Eun Nam, Dae-Hwan Kim, Hyojeong Kim, and Jin-Kyu Kang

Daegu Gyeongbuk Institute of Science and Technology, 50-1 Sang-ri, Hyeonpung-myeon, Dalseong-gun, Daegu 711-873, Republic of Korea

Correspondence should be addressed to Jin-Kyu Kang; apollon@dgist.ac.kr

A new multicarbazole based organic dye (**C2A1**, **C2S1A1**) with a twisted structure was designed and synthesized, and the corresponding dye (**C1A1**) without the twisted structure was synthesized for comparison. They were successfully applied in dye-sensitized solar cells (DSSCs). The results showed that the nonplanar structure of **C2A1** and **C2S1A1** can efficiently retard the dye aggregation and charge recombination. The organic dye (**C2S1A1**) with thiophene units also exhibited a higher molar extinction coefficient and red-shifted absorption, which leads to an improved light harvesting efficiency. The **C2S1A1**-sensitized solar cell produced a solar-to-electricity conversion efficiency of 5.1%, high open circuit voltage (V_{oc}) of 0.69 V, and short-circuit photocurrent density of 10.83 mA cm^{-2} under AM 1.5 irradiation (100 mW cm^{-2}) conditions.

1. Introduction

Since the first successful fabrication of sandwich type solar cells by O'Regan and Grätzel in 1991 [1], the dye-sensitized solar cells (DSSCs) have received significant attention in both the academic and industrial fields, owing to their efficiency, high adaptability, economic feasibility, and relatively less environmental issues compared with the traditional Si-based solar cells. A DSSC consists of three main components: a photoanode, an electrolyte, and a sensitizer. Among these components, the sensitizer plays the important role of capturing the photons and generating the electrons, which are injected into the conduction band of the semiconductor (e.g., TiO$_2$). Significant research efforts have been made to develop efficient sensitizers to enhance the efficiency of DSSCs. Among dyes used as sensitizers, the sensitization of nanocrystalline TiO$_2$ solar cells with Ru-complex photosensitizers (e.g., N3 and N719) has been intensively studied. As a result, power conversion efficiencies (PCEs) higher than 11% under AM 1.5 irradiation have been achieved [2–4]. However, metal-free organic sensitizers have shown PCEs between 6% and 10% [5–9] under the same conditions. Nevertheless, organic

dyes possess many advantages, such as high molar extinction coefficients (ε), ease of customized molecular design for the desired photophysical and photochemical properties, cost effectiveness without the need for transition metals, and in somecases being environmentally friendly. However, one drawback of organic dyes is that the electron lifetimes (τ_e) of the DSSCs with organic dyes were shorter than with a Ru dye. This is due to the charge recombination between the injected electrons in the TiO$_2$ electrode and I$_3^-$ ion in the liquid electrolyte and the aggregation of the dyes on TiO$_2$ (π-π stacking). Usually, charge recombination can be decreased by introducing alkyl side chains into the dye molecule backbones [10, 11], and dye aggregation can be restrained via molecular design that changes the molecular structure from planar to nonplanar or twisted [12–14]. Hence, careful design of dyes containing a twisted structure is a preferred strategy for the development of high performance DSSCs [15–17]. The attachment of a carbazole unit to the conjugated polymer backbone can efficiently depress π-stacking of the polymers in the solid state [18–21], and such a unit has been introduced to the dye molecules used in the DSSCs.

In this study, a new multicarbazole based organic dye (**C2A1** and **C2S1A1**) with a twisted structure was designed and synthesized, and the corresponding dye (**C1A1**) without the twisted structure was synthesized for comparison. The results showed that nonplanar molecular structures prevented charge recombination and dye aggregation. Furthermore, the organic dye (**C2S1A1**) with thiophene units exhibited a higher ε value and red-shifted absorption band because of the improved electron extraction paths from the extension of π-conjugation. All the aforementioned factors contributed to an improved light harvesting ability. To verify the strategy, the photovoltaic performances of the DSSCs containing the dyes were compared using their current-voltage (I-V) curves, monochromatic photon-to-current efficiencies, and impedance spectroscopy (EIS) analysis, which were used to study the interfacial electron transfer process, light harvesting efficiency for photons of particular wavelengths, and estimate τ_e, respectively.

2. Materials and Methods

2.1. Instrumental Analysis. Structural analysis was performed using the ^{1}H NMR spectra recorded on a Bruker Avance NMR 400 spectrometer in CDCl$_3$ and DMSO-d_6. UV/Vis spectra were recorded using a CARY5000 UV/Vis/NIR spectrophotometer. The redox properties were examined by cyclic voltammetry (CV, model: IviumStat). The electrolyte solution of 0.1 M tetrabutylammonium hexafluorophosphate (TBAPF$_6$) was prepared in freshly dried dimethylformamide (CHCl$_3$) solution. The Ag/AgCl and platinum wire (0.5 mm in diameter) electrodes were used as the reference and counter electrodes, respectively.

2.2. Synthesis. All the starting materials and solvents were commercially available and were purchased from Aldrich, TCI, and Alfa Aesar. They were used without further purification. The synthetic procedure of **C1A1**, **C2A2**, and **C2S1A1** is illustrated in Scheme 1.

*2.2.1. Synthesis of 9-Phenyl-9H-carbazole-3-carbaldehyde (**1**).* 9-Phenyl-9H-carbazole (1 g, 8.2 mmol) was dissolved in CHCl$_3$ (in 20 mL) and DMF (1 g, 1.23 mmol). Phosphorus oxychloride (POCl$_3$, 1.9 g, 1.23 mmol) was carefully added through a dropping funnel, while the reaction temperature was maintained below 0°C. After the complete addition of POCl$_3$, the reaction solution turned red color and was stirred under reflux for 8 h. The solution was then poured into water, following which it was neutralized using a sodium hydroxide (NaOH) solution and extracted using methylene chloride (CH$_2$Cl$_2$). The formed precipitate was filtered, dried over magnesium sulfate (MgSO$_4$), and purified using column chromatography on a silica gel with ethyl acetate/hexane as the eluent (1 : 3, v/v). The product was obtained as a pale yellow powder. Yield: (1.3 g, 58.5%). mp ^{1}H NMR (400 MHz, CDCl$_3$): δ 10.1 (s, 1H), 8.14 (s, 1H), 7.67–7.63 (m, 3H), 7.38–7.34 (m, 5H), 6.99–5.86 (m, 3H).

*2.2.2. Synthesis of 2-Cyano-3-(9-phenyl-9H-carbazol-3-yl)-acrylic Acid (**C1A1**).* 9-Phenyl-9H-carbazole-3-carbaldehyde (**1**) (1 g, 3.68 mmol), 2-cyanoacetic acid (0.4 g, 0.48 mmol), and a catalytic amount of piperidine in acetonitrile (CH$_3$CN, 30 mL) were mixed and heated under reflux for 4 h. After the solution was cooled to room temperature, it was poured into ice water. The precipitate was filtered, washed with distilled water, and dried under vacuum. The product was obtained as a yellow powder. Yield: (0.5 g, 40.3%). ^{1}H NMR (400 MHz, DMSO-d_6): δ 8.23 (s, 1H), 8.15–8.13 (m, 4H), 7.71–7.68 (m, 3H), 7.01–6.98 (m, 3H). GC-MS: Calcd. for C$_{22}$H$_{14}$N$_2$O$_2$ m/z: 338.36; found m/z: 338.11[M+H]$^+$; anal. calcd. for C: 78.09; N: 8.28; H: 4.17; found, C: 79.1; N: 8.16; H: 4.84%.

*2.2.3. Synthesis of 9,9′-Diphenyl-9H,9′H-[3,3′]bicarbazolyl (**2**).* 9-Phenyl-9H-carbazole (5 g, 20.5 mmol) was dissolved in 50 mL CHCl$_3$, and iron (III) chloride (15 g, 90 mmol) was added through a dropping funnel at room temperature. After CHCl$_3$ was removed under vacuum, the reaction mixture was poured into methanol (CH$_3$OH), and the obtained yellow solid was filtered. The organic phase was washed with ammonia (NH$_3$), water, and CH$_3$OH. The product was obtained as a yellow powder. Yield: (4.3 g, 90%). ^{1}H NMR (400 MHz, CDCl$_3$): δ 8.44 (d, 2H), 8.23–8.21 (d, 2H), 7.78 (dd, 2H), 7.61–7.53 (m, 8H), 7.50–7.43 (m, 8H), 7.30 (m, 2H).

*2.2.4. Synthesis of 9,9′-Diphenyl-9H,9′H-[3,3′]bicarbazolyl-6-carbaldehyde (**3**).* 9,9′-Diphenyl-9H,9′H-[3,3′]bicarbazolyl (**2**) (2 g, 4.12 mmol) was dissolved in CHCl$_3$ (in 20 mL) and DMF (0.4 g, 5 mmol), and POCl$_3$ (0.75 g, 5 mmol) was carefully added through a dropping funnel, while the reaction temperature was maintained below 0°C. After the complete addition of POCl$_3$, the reaction solution turned red color and was stirred under reflux for 8 h. The mixture was then poured into water. The solution was neutralized using NaOH solution and extracted using CH$_2$Cl$_2$. The formed precipitate was filtered, dried over MgSO$_4$, and purified using column chromatography on a silica gel with ethyl acetate/hexane as the eluent (1 : 1, v/v). The product was obtained as a yellow powder. Yield: (1.3 g, 61.9%). ^{1}H NMR (400 MHz, CDCl$_3$): δ 9.98 (s, 1H), 8.14 (s, 1H), 7.75–7.67 (m, 8H), 7.59–7.5 (m, 8H), 7.35 (m, 5H).

*2.2.5. Synthesis of 2-Cyano-3-(9,9′-diphenyl-9H,9′H-[3,3′]bicarbazolyl-6-yl)-acrylic Acid (**C2A1**).* 9,9′-Diphenyl-9H,9′H-[3,3′]bicarbazolyl-6-carbaldehyde (**3**) (0.8 g, 1.56 mmol), 2-cyanoacetic acid (0.15 g, 1.71 mmol), and a catalytic amount of piperidine in CH$_3$CN (15 mL) were mixed and heated under reflux for 8 h. After the solution was cooled to room temperature, the mixture was poured into ice water. The precipitate was filtered, washed with distilled water, and dried under vacuum. The product was obtained as a dark yellow powder. Yield: (0.4 g, 44.4%). ^{1}H NMR (400 MHz, DMSO-d_6): δ 8.25 (s, 1H), 8.15-8.14 (dd, 4H), 7.84–7.82 (dd, 4H), 7.80–7.78 (m, 4H), 7.61 (d, 4H), 7.40–7.38 (m, 6H). HR-MS (MARDI): Calcd. for C$_{40}$H$_{25}$N$_3$O$_2$ m/z: 579.19; found m/z: 579 [M+H]$^+$; anal. calcd. for C: 82.88; N: 7.25; H: 4.35; found, C: 83.64; N: 7.10; H: 4.48%.
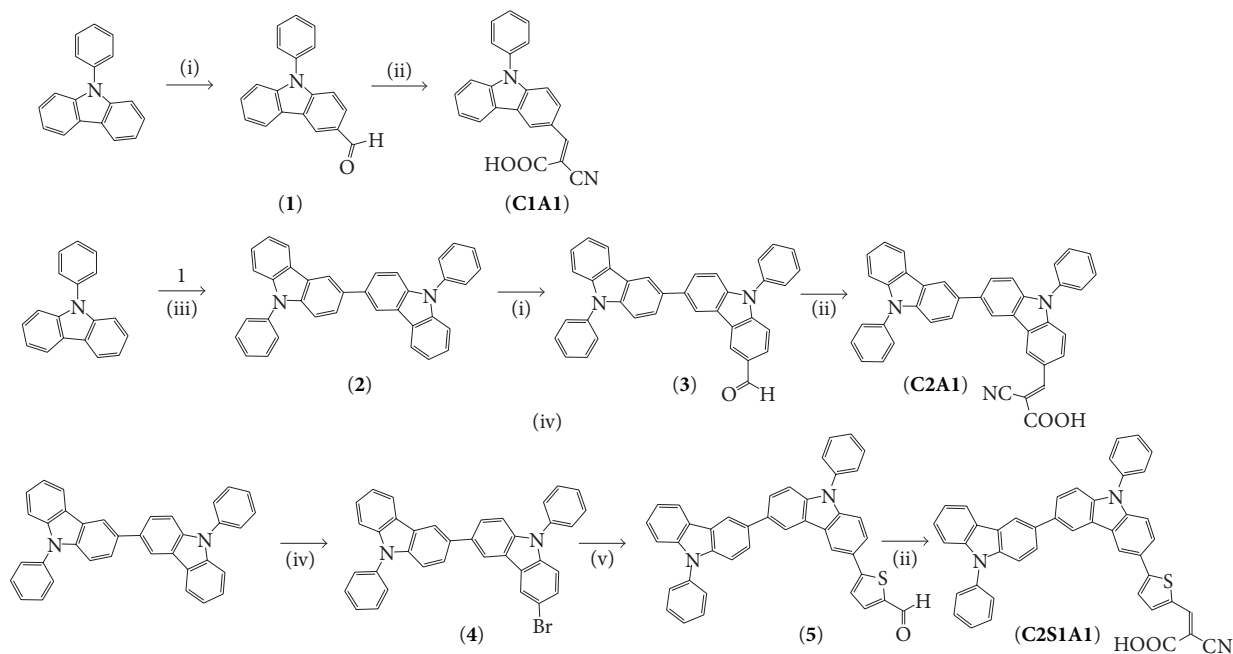
SCHEME 1: Synthetic procedure of organic dyes. (i) DMF, POCl$_3$, and 1,2-dichloroethane, reflux; (ii) cyanoacetic acid, piperidine, and CH$_3$CN, reflux; (iii) FeCl$_3$, CHCl$_3$, and RT; (iv) Br$_2$ and AcOH; and (v) DME, H$_2$O, K$_2$CO$_3$, and 5-formyl-2-thienylboronic acid, reflux.

2.2.6. Synthesis of 6-Bromo-9,9′-diphenyl-9H,9′H-[3,3′]bicarbazolyl (4). Bromine (0.7 g, 4.47 mmol) was slowly added to a solution of 9,9′-diphenyl-9H,9′H-[3,3′]bicarbazolyl (1.97 g, 4.1 mmol) and acetic acid (10 mL) using a syringe. After stirring the mixture at room temperature for 12 h, the reaction was terminated by adding dilute aqueous NaOH (0.1 M). The reaction mixture was extracted using CH$_2$Cl$_2$ and water. The organic layer was separated and dried over anhydrous MgSO$_4$. The crude product was purified by recrystallization using CH$_2$Cl$_2$ and CH$_3$OH. The product was obtained as a red solid. Yield: (1.7 g, 74%). ^{1}H NMR (300 MHz, CDCl$_3$): δ 8.38–8.34 (d, 2H), 7.78–7.76 (m, 4H), 7.65–7.63 (m, 6H), 7.58–7.56 (d, 4H), 7.52–7.47 (m, 4H), 7.31 (m, 3H).

2.2.7. Synthesis of 5-(9,9′-Diphenyl-9H,9′H-[3,3′]bicarbazolyl-6-yl)-thiophene-2-carbaldehyde (5). 6-Bromo-9,9′-diphenyl-9H,9′H-[3,3′]bicarbazolyl (4) (1 g, 1.77 mmol) was dissolved in dimethyl ether (DME, 50 mL), water (in 25 mL), potassium carbonate (K$_2$CO$_3$, 0.6 g, 4.42 mmol), and tetrakis(triphenylphosphine)palladium(0) (Pd (PPh$_3$)$_4$, 0.2 g, 0.18 mmol), and the solution was mixed and heated overnight under reflux. The reaction mixture was poured into water and then extracted using CH$_2$Cl$_2$ and water. The organic phase was washed with brine and dried over MgSO$_4$. The solvent was removed, and the product was purified using column chromatography on a silica gel with CHCl$_3$/hexane as the eluent (1:3, v/v). The product was obtained as a yellow powder. Yield: (0.53 g, 50.4%). ^{1}H NMR (300 MHz, CDCl$_3$): δ 9.61 (s, 1H), δ 8.35–8.32 (d, 4H), 8.15–8.13 (m, 4H), 7.75–7.72 (d, 2H), 7.54–7.49 (m, 6H), 7.49–7.47 (m, 6H), 7.40–7.36 (m, 3H).

2.2.8. Synthesis of 2-Cyano-3-[5-(9,9′-diphenyl-9H,9′H-[3,3′]-bicarbazolyl-6-yl)-thiophen-2-yl]-acrylic Acid (C2A1S1). 5-(9,9′-Diphenyl-9H,9′H-[3,3′]bicarbazolyl-6-yl)-thiophene-2-carbaldehyde (5) (0.5 g, 0.84 mmol), 2-cyanoacetic acid (0.085 g, 1.0 mmol), and a catalytic amount of piperidine in CH$_3$CN (30 mL) were mixed and heated under reflux for 4 h. After the solution was cooled to room temperature, the mixture was poured into ice water. The precipitate was filtered, washed with distilled water, and dried under vacuum. The product was obtained as an orange powder. Yield: (0.28 g, 50.3%). ^{1}H NMR (400 MHz, DMSO-d_6): δ 8.45 (s, 1H), 8.38–8.35 (d, 2H), 8.23–8.21 (m, 3H), 8.19–8.16 (m, 4H), 7.71–7.69 (d, 2H), 7.56–7.51 (m, 6H), 7.49–7.47 (m, 6H), 7.40–7.36 (m, 3H). HR-MS (MARDI): Calcd. for C$_{44}$H$_{27}$N$_3$O$_2$S m/z: 661.18; found m/z: 661.2 [M+H]$^+$; anal. calcd. for C: 79.86; N: 6.35; S: 4.85; H: 4.11; found, C: 80.15; N: 5.98; S: 4.26; H: 4.97%.

2.3. Fabrication and Characterization of DSSCs. The TiO$_2$ paste was coated on a precleaned glass substrate containing fluorine doped tin oxide (FTO, TEC8, Pilkington, 8 Ωcm^{-2}, thickness: 2.3 mm) using the doctor-blade coating method and sintered at 500°C for 1 h. The other TiO$_2$ paste was recoated over the sintered layer using TiO$_2$ particles (approximately 400 nm) as the scattering layer, and the glass substrate was sintered again at 500°C for 1 h. The prepared TiO$_2$ film was dipped in an aqueous solution of 0.04 M titanium tetrachloride (TiCl$_4$) at 70°C for 30 min. For dye adsorption, the annealed TiO$_2$ electrodes were immersed in the dye solution (0.3 mM of dye in ethanol) at room temperature for 24 h. The dye-adsorbed TiO$_2$ electrode and platinum counter electrode were assembled using a 60 μm thick Surlyn (Dupont, 1702)

TABLE 1: Electrochemical parameters of organic dyes.

Dye	ε_{max}[a]/M^{-1} cm^{-1}	λ_{max}[a]/nm (Sol)	E_{0-0}/(eV)[b] (abs)	E_{ox}[c] (V vs. NHE)	$E_{ox} - E_{0-0}$[d] (V vs. NHE)	HOMO (eV)	LUMO (eV)
C1A1	15260	392	2.64	0.84	−1.8	−5.23	−2.59
C2A2	22815	417	2.5	0.68	−1.82	−5.07	−2.57
C2S1A1	26191	442	2.28	0.5	−1.78	−4.89	−2.61

[a]Maximum absorption and extinction coefficient at maximum absorption of dyes in chloroform solution. [b]E_{0-0} (band gap) was determined from intersection of absorption and emission spectra in chloroform solution. [c]Oxidation potential (E_{HOMO}) of dye was measured using cyclic voltammogram in chloroform solution. [d]$E_{HOMO} - E_{0-0} = E_{LUMO}$.
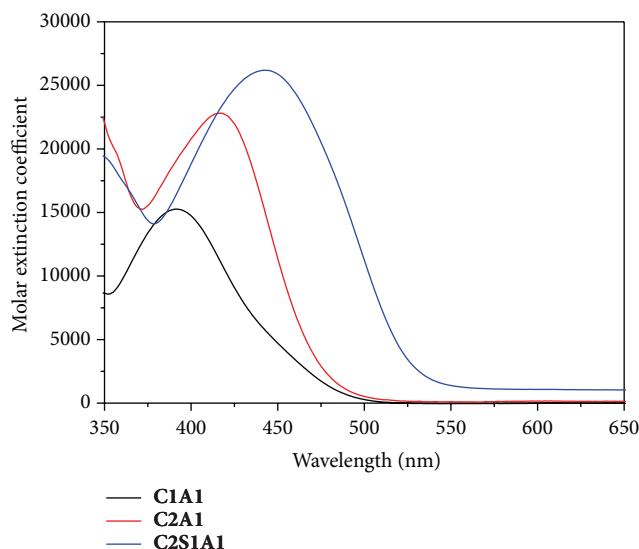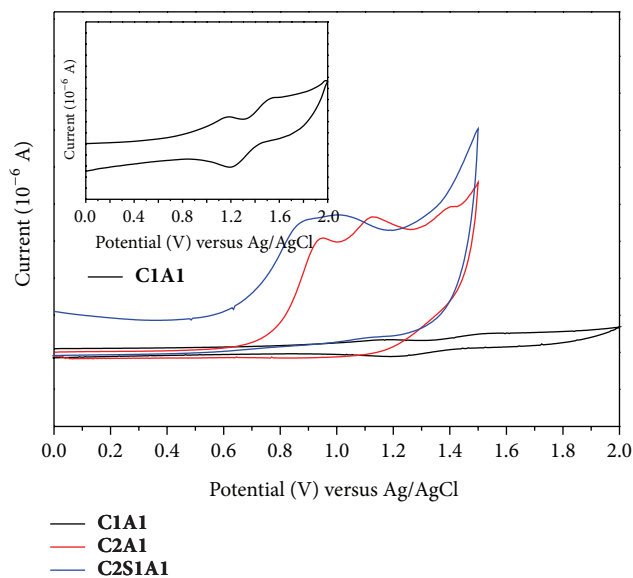

FIGURE 1: Absorption spectra for organic dyes in chloroform solution.

FIGURE 2: The cyclic voltammetric curves of the dyes in chloroform containing 0.1 M TBAPF$_6$ as supporting electrolyte at a scan rate of 50 mV s^{-1}.

as the bonding agent. The liquid electrolyte was introduced through a prepunctured hole on the counter electrode. The electrolyte comprised 3-propyl-1-methyl-imidazolium iodide (PMII, 1 M), lithium iodide (LiI, 0.2 M), iodide (I$_2$, 0.05 M), and *tert*-butylpyridine (TBP, 0.5 M) in CH$_3$CN/valeronitrile (85 : 15). The active areas of the dye-adsorbed TiO$_2$ films were estimated using a digital microscope camera with image analysis software (Moticam 1000).

The photovoltaic *I-V* characteristics of the prepared DSSCs were measured under 1 sunlight intensity (100 mW cm^{-2}, AM 1.5), which was verified using a standard Si-solar cell (Keithley 2400, ORIEL, Newport, PV Measurement Inc.). The monochromatic incident photon-to-current efficiencies (IPCEs) were plotted as a function of the wavelength of light by using an IPCE measurement system (PEC-S20, Peccell Technologies, Inc.).

3. Results and Discussion

3.1. Electronic Absorption Properties of Organic Dyes. The UV/Vis absorption spectra of the organic dyes in CHCl$_3$ are shown in Figure 1 and the corresponding data are summarized in Table 1. The absorption band at 390–450 nm can be attributed to the intramolecular charge transfer (ICT) between the donor and acceptor. The absorption maxima of

the charge-transfer band in CHCl$_3$ are at 392, 417, and 442 nm for **C1A1**, **C2A1**, and **C2S1A1**, respectively. Compared to the **C1A1** dye, the **C2A1** and **C2S1A1** dyes exhibited red-shifted absorption at 25 nm and 50 nm, respectively. This shows that the added carbazole units are beneficial to extend the light absorption and to increase the electron donating ability in comparison to a single carbazole unit (**C1A1**). The ε values of the organic dyes are larger than that of the N719 dye, which indicates that these dyes have good light harvesting ability.

The electrochemical behavior of the organic dyes was measured by CV, as shown in Figure 2. The detailed data are listed in Table 1. The highest occupied molecular orbital (HOMO) levels of these dyes were 0.84 V, 0.68 V, and 0.5 V for **C1A1**, **C2A1**, and **C2S1A1** versus normal hydrogen electrode (NHE), respectively. The obtained values are more positive than the I$_3^-$/I$^-$ redox potential value (0.4 V versus NHE). This indicates that the oxidized dyes formed after the electron injection into the conduction band of TiO$_2$ could accept electrons from the electrolyte thermodynamically. They could also accept electrons from the LUMO levels that are more negative than the TiO$_2$ conduction band. This indicates that the electrons from the excited LUMO level can be easily injected onto the photoelectrode and that the oxidized dyes may be regenerated using the I$_3^-$/I$^-$ redox couple.
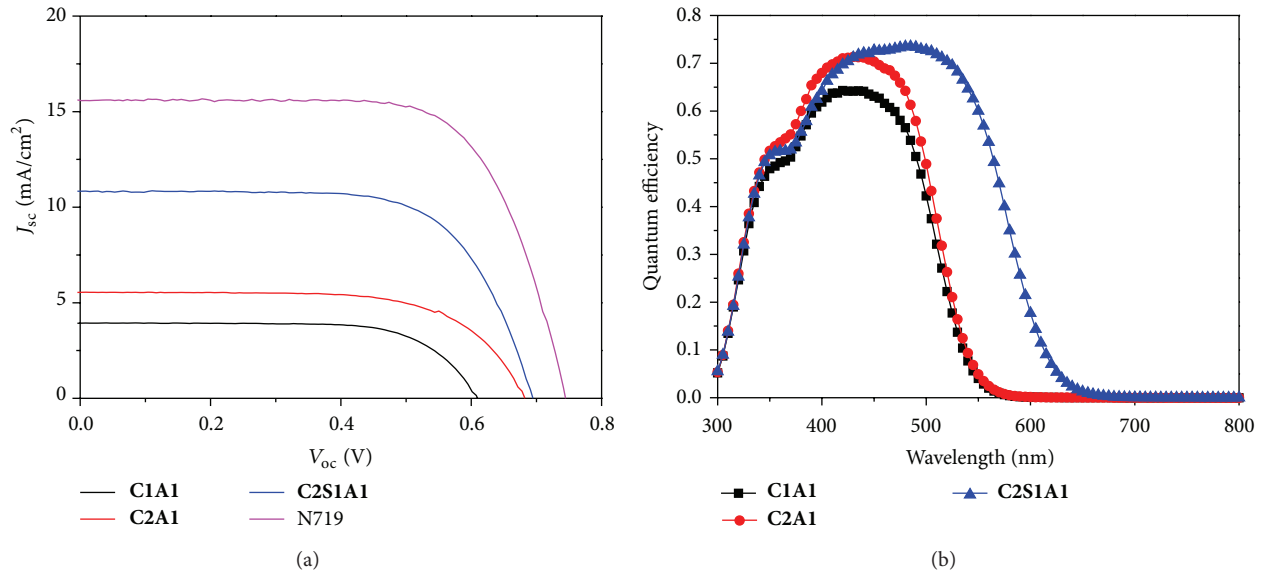
(a)

(b)

FIGURE 3: (a) Current density-voltage characteristics of dye-sensitized solar cells containing organic dyes under illumination using simulated solar light (AM 1.5, 100 mW cm^{-2}). (b) Incident photon-to-current efficiency curves for dye-sensitized solar cells containing organic dyes.

3.2. Photovoltaic Measurements. The photovoltaic performances of the DSSCs based on organic dyes were compared using the variation of flow current with the bias voltage, IPCE, impedance, and electron lifetime analysis. Figure 3(a) shows the I-V curves of the DSSCs with the different organic dyes, as summarized in Table 2.

Under the standard global AM 1.5 solar irradiation, the cells based on **C2A1S1** and **C2A1** dyes containing two carbazole units exhibited higher efficiency compared to those based on the **C1A1** dye. The short-circuit current density (J_{sc}), open circuit voltage (V_{oc}), and overall yield (η) of the three dyes are in the order of **C2S1A1** > **C2A1** > **C1A1**. This is due to the improved light absorption ability by the added carbazole units and the existence of twisted structures, which resulted in an increased current density and inhibited dye aggregation and charge recombination [22]. The higher efficiency of the **C2S1A1** dye can be explained by the increased electron donating ability and ε values due to the introduction of thiophene. The thiophene unit in the **C2S1A1** dye may have caused strong π-π interactions that could be attributed to the light harvesting efficiency.

In order to rationalize these observations, the spectra of the monochromatic IPCE of the DSSCs based on the organic dyes are shown in Figure 3(b). The carbazole-based sensitizers efficiently converted visible light to photocurrent across the higher energy region over the wavelength range of 350–550 nm. A maximum IPCE of 74% was realized at 480 nm for the **C2S1A1** dye, while the **C2A1** and **C1A1** dyes exhibited a maximum IPCE of 69% and 63% at 440 nm, respectively. This is probably due to the fact that the **C2S1A1** dye has a much broader absorption spectrum whose contributions are expected to enhance the photogenerated current values.

In addition, EIS was employed to study the electron recombination in the DSSCs. The EIS measurement is shown

TABLE 2: Photovoltaic performance of dye-sensitized solar cells[a].

Dye[b]	J_{sc}/mA cm^{-2}	V_{oc}/V	FF (%)	η/%
C1A1	3.939	0.608	69.84	1.67
C2A1	5.548	0.681	66.04	2.5
C2S1A1	10.83	0.69	67.68	5.1
N719	15.58	0.745	69.66	8.09

[a]Photovoltaic performance under AM1.5 irradiation of dye-sensitized solar cells containing organic dyes based on 3-propyl-1-methyl-imidazolium iodide (1 M), lithium iodide (0.2 M), iodide (0.05 M), and *tert*-butylpyridine (0.5 M) in acetonitrile/valeronitrile (85 : 15). [b]Dye bath: chloroform solution (3×10^{-4} M).

in Figure 4, and the data is listed in Table 3. The R_{s} and R_{rec} represent the series resistance and charge-transfer resistance at the dye/TiO$_2$/electrolyte interface, respectively, and R_{CE} represents the resistance at the counter electrode. The values of R_{s} and R_{CE} (the first semicircle in the Nyquist plot) were almost the same for the three dyes because of the same electrode material and same electrolyte used. The R_{rec} was determined by the middle semicircle in the Nyquist plot. From the EIS measurements, the τ_{e}, which expresses the electron recombination between the electrolyte and TiO$_2$, was calculated following a literature procedure [23]. The R_{rec} for the dyes **C1A1**, **C2A1**, and **C2S1A1** was 36.65, 19.71, and 13.84 Ω, respectively. Under illumination, the smaller R_{rec} values indicated fast charge generation and transport. The calculated τ_{e} of **C1A1**, **C2A1**, and **C2S1A1** was 2.36, 3.52, and 4.7 ms, respectively. Among the dyes, the **C2S1A1**-based cell had a longer τ_{e}, which led to a lower rate of charge recombination and thus improved V_{oc}. Therefore, the **C2S1A1** dye provided a much faster electron transport and prolonged τ_{e}. The improved values of J_{sc} and V_{oc} of the DSSCs with the **C2S1A1** dye can be mainly attributed to the improved light harvesting efficiency.
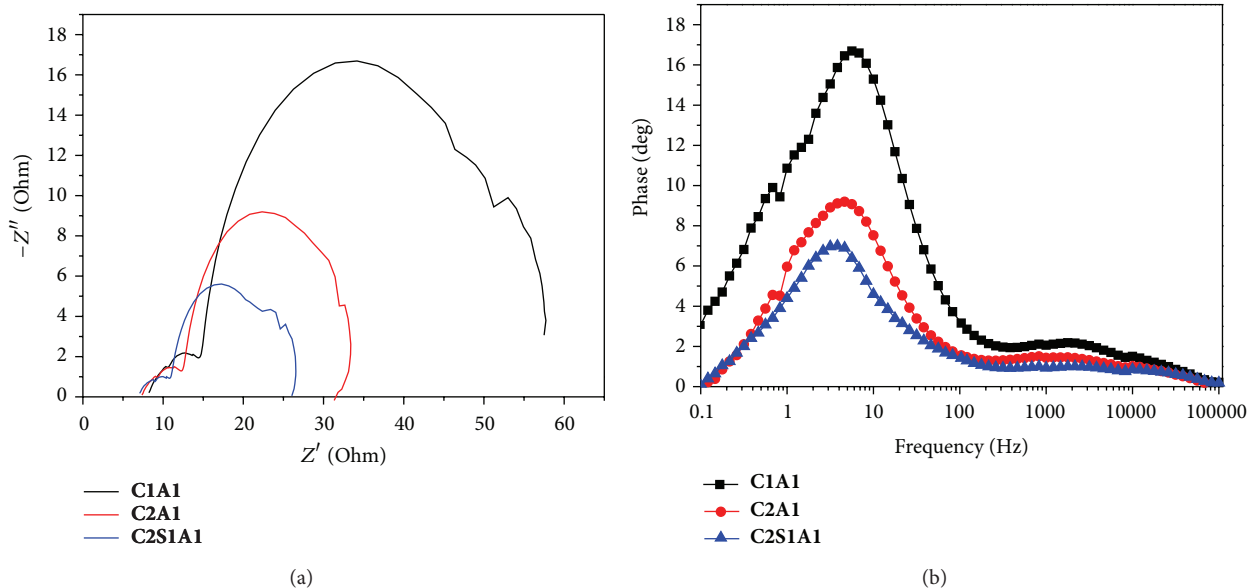
(a)

(b)

FIGURE 4: (a) Measured dye-sensitized solar cell impedance spectrum at forward bias condition under illumination. (b) Bode-phase plots for the dye-sensitized solar cells.

TABLE 3: Performances of mercurochrome and organic dye based dye-sensitized solar cells and electron transport properties of their photoanodes as determined by impedance analysis. Cell areas are 0.24 cm^2.

Dyes	R_1 (Ω)[a]	R_2 (Ω)[b]	R_3 (Ω)[c]	τ_e[d] (ms)
C1A1	8.29	6.32	36.65	2.4
C2A1	7.41	5.1	19.71	3.5
C2S1A1	6.97	3.99	13.84	4.7

[a] R_1 is fluorine doped tin oxide interface resistance. [b] R_2 is due to resistance at interface between counter electrode and electrolyte. [c] R_3 possibly originated from backward charge transfer from TiO_2 to electrolyte and electron conduction in porous TiO_2 film. [d] τ is lifetime of an electron in dye-sensitized solar cells.

4. Conclusions

In this study, a new multicarbazole based organic dye (**C2A1** and **C2S1A1**) with a twisted structure was designed and synthesized, and the corresponding dye (**C1A1**) without twisted structure was synthesized for comparison. The addition of carbazole units to the organic dyes is an effective method to adjust and control the photochemical and electrochemical properties of the dyes, which determine the charge recombination and overall energy conversion efficiency. The **C2S1A1** dye exhibited the highest PCE of 5.1% with a V_{oc} of 0.69 V and short-circuit photocurrent density of 10.83 mA cm^{-2}. The increased electron donating ability of the **C2S1A1** molecule provided higher ε values and a much broader absorption spectrum.

Conflict of Interests

The authors declare that there is no conflict of interests regarding the publication of this paper.
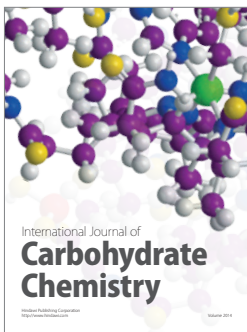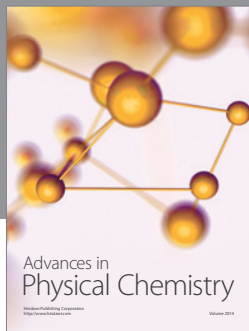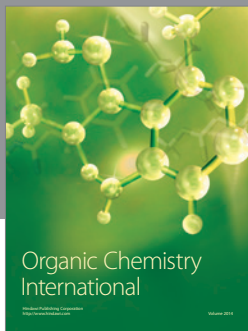
References

[1] B. O'Regan and M. Grätzel, "A low-cost, high-efficiency solar cell based on dye-sensitized colloidal TiO$_2$ films," *Nature*, vol. 353, pp. 737–740, 1991.

[2] M. K. Nazeeruddin, S. M. Zakeeruddin, R. Humphry-Baker et al., "Acid-base equilibria of (2,2′-bipyridyl-4,4′-dicarboxylic acid)ruthenium(II) complexes and the effect of protonation on charge-transfer sensitization of nanocrystalline titania," *Inorganic Chemistry*, vol. 38, no. 26, pp. 6298–6305, 1999.

[3] M. K. Nazeeruddin, F. de Angelis, S. Fantacci et al., "Combined experimental and DFT-TDDFT computational study of photoelectrochemical cell ruthenium sensitizers," *Journal of the American Chemical Society*, vol. 127, no. 48, pp. 16835–16847, 2005.

[4] M. J. Grätzel, "Dye-sensitized solar cells," *Journal of Photochemistry and Photobiology C: Photochemistry Reviews*, vol. 4, no. 2, pp. 145–153, 2003.

[5] T. Horiuchi, H. Miura, K. Sumioka, and S. Uchida, "High efficiency of dye-sensitized solar cells based on metal-free indoline dyes," *Journal of the American Chemical Society*, vol. 126, no. 39, pp. 12218–12219, 2004.

[6] Z. Wang, Y. Cui, K. Hara, Y. Dan-Oh, C. Kasada, and A. Shinpo, "A high-light-harvesting-efficiency coumarin dye for stable dye-sensitized solar cells," *Advanced Materials*, vol. 19, no. 8, pp. 1138–1141, 2007.

[7] K. Hara, T. Sato, R. Katoh et al., "Molecular design of coumarin dyes for efficient dye-sensitized solar cells," *The Journal of Physical Chemistry B*, vol. 107, no. 2, pp. 597–606, 2003.

[8] S. Hwang, J. H. Lee, C. Park et al., "A highly efficient organic sensitizer for dye-sensitized solar cells," *Chemical Communications*, no. 46, pp. 4887–4889, 2007.

[9] S. S. Park, Y. S. Won, Y. C. Choi, and J. H. Kim, "Molecular design of organic dyes with double electron acceptor for dye-sensitized solar cell," *Energy & Fuels*, vol. 23, no. 7, pp. 3732–3736, 2009.

[10] J. E. Kroeze, N. Hirata, S. Koops et al., "Alkyl chain barriers for kinetic optimization in dye-sensitized solar cells," *Journal of the American Chemical Society*, vol. 128, pp. 16376–16383, 2006.

[11] J. He, W. Wu, J. Hua et al., "Bithiazole-bridged dyes for dye-sensitized solar cells with high open circuit voltage performance," *Journal of Materials Chemistry*, vol. 21, pp. 6054–6062, 2011.

[12] L. Y. Lin, C. H. Tsai, K. T. Wong et al., "Organic dyes containing coplanar diphenyl-substituted dithienosilole core for efficient dye-sensitized solar cells," *The Journal of Organic Chemistry*, vol. 75, no. 14, pp. 4778–4785, 2010.

[13] N. Cho, H. Choi, D. Kim et al., "Novel organic sensitizers containing a bulky spirobifluorene unit for solar cell," *Tetrahedron*, vol. 65, no. 31, pp. 6236–6243, 2009.

[14] D. Heredia, J. Natera, M. Gervaldo et al., "Spirobifluorene-bridged donor/acceptor dye for organic dye-sensitized solar cells," *Organic Letters*, vol. 12, no. 1, pp. 12–15, 2010.

[15] Y. Liang, B. Peng, J. Liang, Z. Tao, and J. Chen, "Triphenylamine-based dyes bearing functionalized 3,4-propylenedioxythiophene linkers with enhanced performance for dye-sensitized solar cells," *Organic Letters*, vol. 12, no. 6, pp. 1204–1207, 2010.

[16] X. Zhang, Z. Wang, Y. Cui, N. Koumura, A. Furube, and K. Hara, "Organic sensitizers based on hexylthiophene-functionalized indolo[3, 2-b]carbazole for efficient dye-sensitized solar cells," *Journal of Physical Chemistry C*, vol. 113, no. 30, pp. 13409–13415, 2009.

[17] J. I. Nishida, T. Masuko, Y. Cui et al., "Molecular design of organic dye toward retardation of charge recombination at semiconductor/dye/electrolyte interface: introduction of twisted π-linker," *Journal of Physical Chemistry C*, vol. 114, no. 41, pp. 17920–17925, 2010.

[18] E. M. Barea, C. Zafer, B. Gultekin et al., "Quantification of the effects of recombination and injection in the performance of dye-sensitized solar cells based on N-substituted carbazole dyes," *Journal of Physical Chemistry C*, vol. 114, no. 46, pp. 19840–19848, 2010.

[19] Z. J. Ning, Q. Zhang, W. J. Wu, H. C. Pei, B. Liu, and H. J. Tian, "Starburst triarylamine based dyes for efficient dye-sensitized solar cells," *The Journal of Organic Chemistry*, vol. 73, pp. 3791–3797, 2008.

[20] D. Kim, J. K. Lee, S. O. Kang, and J. Ko, "Molecular engineering of organic dyes containing N-aryl carbazole moiety for solar cell," *Tetrahedron*, vol. 63, no. 9, pp. 1913–1922, 2007.

[21] N. Koumura, Z. S. Wang, S. Mori, M. Miyashita, E. Suzuki, and K. Hara, "Alkyl-functionalized organic dyes for efficient molecular photovoltaics," *Journal of the American Chemical Society*, vol. 128, no. 44, pp. 14256–14257, 2006.

[22] H. Lai, J. Hong, P. Liu, C. Yuan, Y. Li, and Q. Fang, "Multicarbazole derivatives: New dyes for highly efficient dye-sensitized solar cells," *RSC Advances*, vol. 2, no. 6, pp. 2427–2432, 2012.

[23] L. C. Zou and C. Hunt, "Characterization of the conduction mechanisms in adsorbed electrolyte layers on electronic boards using AC impedance," *Journal of the Electrochemical Society*, vol. 156, no. 1, pp. C8–C15, 2009.